

# THE COMPLEX ARCHITECTURE OF OXYGENIC PHOTOSYNTHESIS

*Nathan Nelson and Adam Ben-Shem*

**Abstract** | Oxygenic photosynthesis is the principal producer of both oxygen and organic matter on earth. The primary step in this process — the conversion of sunlight into chemical energy — is driven by four, multisubunit, membrane-protein complexes that are known as photosystem I, photosystem II, cytochrome  $b_6f$  and F-ATPase. Structural insights into these complexes are now providing a framework for the exploration not only of energy and electron transfer, but also of the evolutionary forces that shaped the photosynthetic apparatus.

**PROTONMOTIVE FORCE** (pmf). A special case of an electrochemical potential. It is the force that is created by the accumulation of protons on one side of a cell membrane. This concentration gradient is generated using energy sources such as redox potential or ATP. Once established, the pmf can be used to carry out work, for example, to synthesize ATP or to pump compounds across the membrane.

Oxygenic photosynthesis — the conversion of sunlight into chemical energy by plants, green algae and cyanobacteria — underpins the survival of virtually all higher life forms. The production of oxygen and the assimilation of carbon dioxide into organic matter determines, to a large extent, the composition of our atmosphere and provides all life forms with essential food and fuel. The study of the photosynthetic apparatus is a prime example of research that requires a combined effort between numerous disciplines, which include quantum mechanics, biophysics, biochemistry, molecular and structural biology, as well as physiology and ecology. The time courses that are measured in photosynthetic reactions range from femtoseconds to days, which again highlights the complexity of this process.

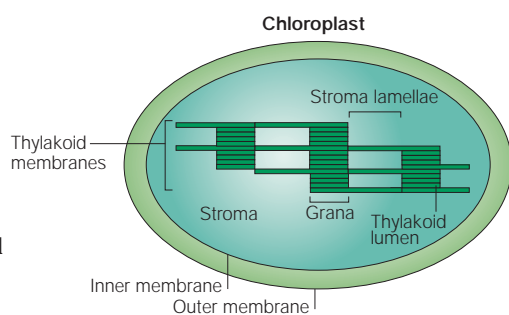
Plant photosynthesis is accomplished by a series of reactions that occur mainly, but not exclusively, in the chloroplast (BOX 1). Initial biochemical studies showed that the chloroplast thylakoid membrane is capable of light-dependent water oxidation, NADP reduction and ATP formation<sup>1</sup>. Biochemical and biophysical studies<sup>2–6</sup> revealed that these reactions are catalysed by two separate photosystems (PSI and PSII) and an ATP synthase (F-ATPase): the latter produces ATP at the expense of the PROTONMOTIVE FORCE (pmf) that is formed by the light reaction. The cytochrome- $b_6f$  complex mediates electron transport between PSII and PSI and converts the redox energy into a high-energy intermediate (pmf) for ATP formation<sup>7</sup>.

After the invention of SDS-PAGE<sup>8,9</sup>, the biochemical composition of the four multisubunit protein complexes began to be elucidated<sup>10–14</sup>. According to the partial reactions that they catalyse, PSII is defined as a water-plastoquinone oxidoreductase, the cytochrome- $b_6f$  complex as a plastoquinone-plastocyanin oxidoreductase, PSI as a plastocyanin-ferredoxin oxidoreductase and the F-ATPase as a pmf-driven ATP synthase<sup>15</sup> (FIG. 1). PSI and PSII contain chlorophylls and other pigments that harvest light and funnel its energy to a reaction centre. Energy that has been captured by the reaction centre induces the excitation of specialized reaction-centre chlorophylls (PRIMARY ELECTRON DONORS; a special chlorophyll pair in PSI), which initiates the translocation of an electron across the membrane through a chain of cofactors. Water, the electron donor for this process, is oxidized to  $O_2$  and 4 protons by PSII. The electrons that have been extracted from water are shuttled through a quinone pool and the cytochrome- $b_6f$  complex to plastocyanin, a small, soluble, copper-containing protein<sup>16</sup>. Solar energy that has been absorbed by PSI induces the translocation of an electron from plastocyanin at the inner face of the membrane (thylakoid lumen) to ferredoxin on the opposite side (stroma; FIG. 1). The reduced ferredoxin is subsequently used in numerous regulatory cycles and reactions, which include nitrate assimilation, fatty-acid desaturation and NADPH production. The CHARGE SEPARATION in PSI and PSII, together with the electron transfer through the cytochrome- $b_6f$  complex, leads to the

Department of  
Biochemistry,  
The George S. Wise  
Faculty of Life Sciences,  
Tel Aviv University,  
Tel Aviv 69978, Israel.  
Correspondence to N.N.  
e-mail:  
nelson@post.tau.ac.il  
doi:10.1038/nrm1525

## Box 1 | The basic features of higher plant chloroplasts

**Chloroplasts (see figure) are organelles that are bound by a double membrane and are found in the cells of green plants and algae in which photosynthesis takes place. They contain a third membrane system that is known as thylakoids, where all the pigments, electron-transport complexes and the ATP synthase (F-ATPase) are located. The thylakoid membranes of higher plants consist of stacks of membranes that form the so-called granal regions. Adjacent grana are connected by non-stacked membranes called stroma lamellae. The fluid compartment that surrounds the thylakoids is known as the stroma, and the space inside the thylakoids is known as the lumen.**



## PRIMARY ELECTRON DONORS

Reaction-centre chlorophyll pairs ( $P_{700}$  in PSI and  $P_{680}$  in PSII) that are very different from antenna chlorophylls. When they receive light energy (from the antenna pigments), they generate a redox-active chemical species. Excited  $P_{680}^*$  donates an electron to another component of PSII, then eventually to the cytochrome- $b_6/f$  complex and to PSI. After donating the electron,  $P_{680}^+$  — the strongest oxidant in biology — is generated.  $P_{700}^*$  is the strongest reductant in biology.  $P_{700}^+$  accepts an electron from plastocyanin.

## CHARGE SEPARATION

The process in which excited  $P_{680}^*$  and  $P_{700}^*$  donate their electrons to their respective acceptors to generate  $P_{680}^+$  and  $P_{700}^+$ , respectively.

## ELECTROCHEMICAL POTENTIAL

Electrochemical potential is the sum of the chemical potential (concentration difference across the membrane) and the electrical potential (charge-concentration difference across the membrane).

## QUANTUM YIELD

In a particular system, the number of defined electronic or chemical events that occur per photon absorbed.

## QUANTA

Specific packets of electromagnetic energy (also known as photons). They have no mass, but they do have a momentum. Photosynthetic organisms capture the momentum of a photon and translate it into biological energy.

formation of an ELECTROCHEMICAL-POTENTIAL gradient (the pmf), which powers ATP synthesis by the fourth protein complex, F-ATPase<sup>17</sup>. In the dark,  $CO_2$  reduction to carbohydrates is fuelled by ATP and NADPH<sup>18</sup>.

All of the four protein complexes that are necessary for the light-driven reactions of photosynthesis reside in the chloroplast, in a membrane continuum of flattened vesicles called thylakoids (FIG. 1a; see also the BOX 1 figure). In higher plants, thylakoids are differentiated into two distinct membrane domains — the cylindrical stacked structures known as grana and the interconnecting single-membrane regions called stroma lamellae. The four membrane complexes that drive the light reaction are not evenly distributed throughout thylakoids: PSI localizes to the stroma lamellae and is segregated from PSII, which is almost exclusively found in the grana; F-ATPase concentrates mainly in the stroma lamellae, whereas the cytochrome- $b_6/f$  complex preferentially populates the grana and the grana margins<sup>19</sup> (FIG. 1a). The recent determination of the structures of these complexes — or in the case of F-ATPase, of a close homologue from mitochondria — completes the description of the architecture of energy transduction in oxygenic photosynthesis that has been sought for the past 50 years (FIG. 1b). Here, we describe some of the functional implications that have emerged from these structures and discuss their importance in addressing key issues in photosynthetic research.

The two photosystems and electron transfer  
As mentioned above, PSI and PSII contain numerous pigments that harvest light and funnel the excitation to the primary electron donors, which can reduce an electron acceptor and accept electrons from specific electron donors. The two photosystems therefore function as Einstein's photoelectric machines (BOX 2), which have evolved to operate with a high QUANTUM YIELD that is unmatched by any biological or chemical system. However, although PSI operates with an almost perfect quantum yield of 1.0, PSII operates with a lower quantum yield of about 0.85 (REF. 20). Because sunlight is abundant, the difference in quantum yield seems

unimportant. However, the lost QUANTA can inflict damage on the photosynthetic complexes. In the less efficient PSII, one of the subunits, D1, is turned over so fast that its synthesis represents 50% of the total protein synthesis in chloroplasts, even though D1 actually represents only ~0.1% of the total protein composition of chloroplasts<sup>21,22</sup>. Knowledge of the structures of, and pigment distributions in, PSI and PSII should eventually help us to explain the differences in their quantum yields and the consequences of these differences. In the following sections, we review the contribution of recent structural data to our understanding of the architecture and function of oxygenic photosynthesis.

## Photosystem II

The PSII reaction centre is composed of two similar ~40-kDa proteins (D1 and D2), which each consist of 5 transmembrane helices, and these proteins coordinate both the manganese cluster of PSII and all of the electron-transfer components<sup>23</sup> (FIG. 2a). Flanking the reaction centre are the intrinsic light-harvesting proteins CP43 and CP47, which each consist of 6 transmembrane helices and bind 14 and 16 chlorophyll-a molecules<sup>24</sup>, respectively. However, most of the chlorophylls that are associated with PSII are harboured in the extrinsic, peripheral light-harvesting complex II (LHCII) antenna complexes. These are trimers of the light-harvesting proteins Lhcb1, Lhcb2 and Lhcb3, although each trimer can contain different stoichiometries of these proteins. The Lhcb proteins have a similar structure, and harbour 12–14 chlorophyll-a and -b molecules and up to 4 CAROTENOIDS<sup>25,26</sup>. The number of trimers that are associated with PSII varies with irradiance level. Energy transfer from LHCII to CP43/CP47 or D1/D2 is mediated by the minor light-harvesting proteins Lhcb6 (CP24), Lhcb5 (CP26) and Lhcb4 (CP29), each of which is similar to an LHCII monomer. The organization of the Lhcb proteins with the PSII reaction centre has been extensively studied using electron microscopy and several low-resolution models have been described<sup>27,28</sup>.

PSII catalyses a unique process of water oxidation and provides almost all of the earth's oxygen. Although some inorganic chemical reactions can do a similar job, these reactions are so violent that biological processes would not be able to tolerate them. The evolution of PSII was therefore absolutely crucial for the emergence and endurance of aerobic organisms. The mechanism of oxygen production involves the oxidation of two water molecules to make molecular oxygen ( $O_2$ ) in a combined mechanism that requires the absorption of four light quanta. Two weakly coupled chlorophylls known as  $P_{680}$  function as the primary electron donor (680 nm is the peak of the lowest-energy absorption band of  $P_{680}$ ). After absorption of the first of the light quanta, an electron is translocated from  $P_{680}$  through an accessory chlorophyll and a pheophytin molecule to the tightly bound quinone  $Q_A$ , and this is followed by the reduction of a mobile quinone  $Q_B$  (FIG. 2b). The oxidized  $P_{680}^+$ , which has the highest REDOX POTENTIAL observed in a biological system (> 1 V), oxidizes a nearby tyrosine ( $Y_2$ ).  $Y_2$  then extracts

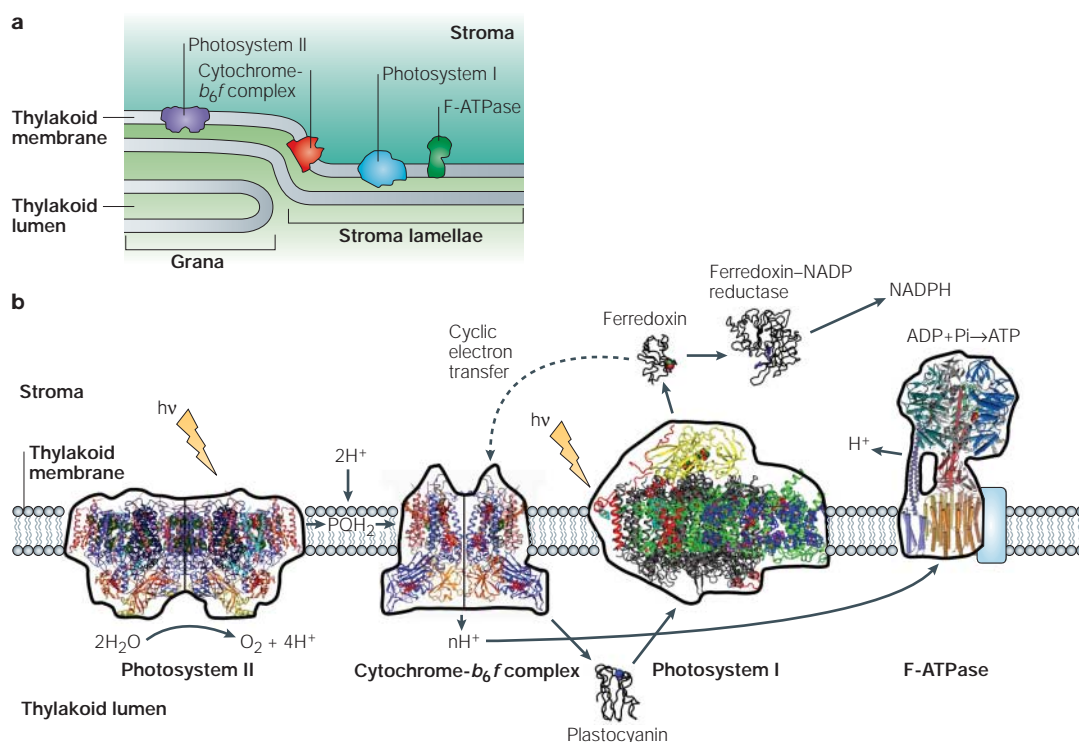


**Figure 1 | The structures of the four large membrane-protein complexes in thylakoid membranes that drive oxygenic photosynthesis. a** | A schematic depiction of the distribution of the four protein complexes in the thylakoid membranes of chloroplasts. **b** | The available structural data for these membrane-protein complexes, which have been adjusted to the relative size of plant photosystem I. The outlines around these complexes illustrate the basic structural knowledge that was available before crystallization studies. Inside these outlines are structures of photosystem II (REF. 24), the cytochrome-*b*<sub>6</sub>*f* complex<sup>47</sup> and photosystem I (REF. 62), and a structural model of F-ATPase, which was created from the available partial structures by W. Frasch (Arizona State University, Arizona, USA). The structures of some of the electron donors and acceptors are also shown (for example, plastocyanin<sup>83</sup> and ferredoxin<sup>82</sup>), and the principal electron and proton pathways are indicated. A lightning bolt symbolizes the light quanta (hv) that are absorbed by PSII and PSI, and a cyclic electron-transfer pathway is indicated by a dashed line. Pi, inorganic phosphate.

#### CAROTENOID

Any of a class of yellow to red pigments, which include carotenes and xanthophylls.

#### REDOX POTENTIAL

Redox potential is a measure (in volts) of the affinity of a substance for electrons. This value for each substance is compared to that for hydrogen, which is set arbitrarily at zero. Substances that are more strongly oxidizing than hydrogen have positive redox potentials (oxidizing agents), whereas substances that are more reducing than hydrogen have negative redox potentials (reducing agents).

#### KOK-JOLIOT FIVE S-STATES

The oxidation of water to oxygen occurs at the oxygen-evolving complex/manganese cluster in photosystem II. This cluster cycles through five states ( $S_0$ – $S_4$ ) during the oxidation process, and this cycle was discovered by Bessel Kok and Pierre Joliot about four decades ago.

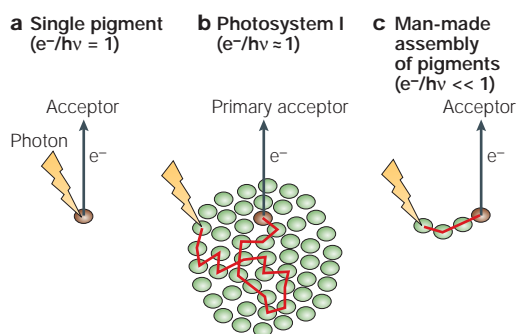
an electron (and perhaps a proton) from a cluster of four manganese ions, which binds two substrate water molecules and has a calcium ion, a chloride ion and a bicarbonate ion as necessary cofactors. After another photochemical cycle, the doubly reduced  $Q_B$  ( $Q_B^{2-}$ ) takes up two protons from the stroma to form  $Q_BH_2$  and is released into the lipid bilayer to be replaced by an oxidized quinone from the membrane quinone pool. This pool consists of oxidized (PQ) and reduced ( $PQH_2$ ) plastoquinones (plastoquinone, rather than quinone, is specified when it is the predominant quinone). After two more photochemical cycles, the manganese cluster is provided with a total of four oxidizing equivalents, which are used to oxidize two water molecules to produce  $O_2$ . The manganese cluster is then reset to its initially reduced state, which is designated  $S_0$  in the KOK-JOLIOT FIVE S-STATES reaction ( $S_0$ – $S_4$ ). In the past, several mechanisms have been proposed to explain this oxygen-production process, and numerous elegant experiments were carried out to further our understanding of it<sup>29–31</sup>. However, it was clear that only a complete description of the spatial distribution of the metal ions involved, as well as of their immediate environment, would allow the mechanism to be fully understood at the molecular level.

Crystal structures of PSII from two different cyanobacteria have shed light on the location of the manganese cluster — or oxygen-evolving cluster — and provided a coarse view of it<sup>32,33</sup>. Recently, a higher resolution structure, aided by the analysis of the anomalous diffraction pattern of the occupied metal-binding sites, provided a more detailed description of the manganese cluster and assigned, for the first time, almost all of the amino-acid side chains involved<sup>24</sup>. Three manganese ions and one calcium ion form a cube-like cluster, in which the metal ions are bridged by four mono-oxygen atoms. One of these oxygens connects the cluster to a fourth manganese ion, which is designated Mn4 (FIG. 2b). The latter is also linked to the calcium ion by a putative bicarbonate ion, which fits with the proposal that this anion is involved in manganese-cluster assembly. The 3 + 1 arrangement of the manganese ions — which agrees with EXAFS (extended, X-ray absorption, fine structure) measurements — and the proximity of the calcium ion to Mn4, support a model in which only one of the manganese ions, namely Mn4, binds a water molecule as a substrate and extracts electrons from it<sup>24,34,35</sup>. It was proposed that immediately before the formation of the O=O bond, the Mn4 ion becomes

## Box 2 | Photosystem I — an almost perfect 'Einstein photochemical machine'

Light seems to travel as either a wave or a particle, depending on how you happen to be looking at it. When it travels as a particle, the little particles of energy are called photons, and these little packets (quanta) of electromagnetic radiation have a measurable and known amount of energy, and also a wavelength. When a pigment molecule absorbs light energy, it is absorbing photons.

This extra energy raises the energy level of the atoms — they get 'excited' and the electrons become more energized. According to Einstein's photoelectric law (that resulted in him being awarded the Nobel Prize for Physics in 1921), the absorption of one photon ( $h\nu$ ) will excite one electron ( $e^-$ ) to a higher energy level, and the quantum yield of this process is 1.0 (for each absorbed photon, one electron will jump to a higher energy level; see figure, part a). In photosynthesis, the energized (or excited) electrons can move from the pigments to electron acceptors to provide energy for the photosynthetic process. Plant photosystem I (PSI) contains more than 200 pigments. Each of them could absorb a photon and the excitation could transitionally travel through several hundred pigments before it will elevate the energy level of a single electron in a special chlorophyll pair called  $P_{700}$ . This process has an unprecedented quantum yield of nearly 1.0, so we define PSI as an almost perfect 'Einstein photochemical machine' (see figure, part b). This high quantum yield could not be achieved by any man-made assembly of pigments (see figure, part c). Understanding the mechanism of energy migration in PSI might, in the future, lead to the synthesis of a perfect, man-made Einstein photochemical machine.



highly oxidative, probably producing an Mn(V) state (REF. 24). The O=O bond might then be formed by a nucleophilic attack on the electron deficient Mn(V)=O by a second water molecule that is ligated to the nearby calcium ion, as proposed by Brudvig and colleagues<sup>30</sup>. The role of the other manganese ions is not fully understood, but they probably contribute to orientating the water molecules and stabilizing the cluster. An even higher-resolution structure is required to ascertain the validity of the proposed arrangement and the exact location of the bridging monooxygens, as well as to complete the partial list of ligands that must be coordinated by the metal ions. These probably include water and chloride ions (REF. 36), which are not present in the reported structure<sup>24</sup>. Only when we have an increased resolution, and perhaps structures of PSII that are locked in different S states, will a more complete understanding of arguably the most important chemical reaction on earth be possible.

When electron extraction from water is impaired (for example, under low-temperature conditions), the longer-lived  $P_{680}^+$  state might extract electrons from its surroundings and therefore cause damage. However, the structure of PSII supports the idea that, under such conditions, an electron might be donated to  $P_{680}^+$  by an alternative electron-transfer pathway that involves cytochrome  $b_{559}$ , a carotenoid and a chlorophyll at the periphery of the reaction centre (FIG. 2b), and perhaps several chlorophylls of the CP43 subunit. Electrons might be injected into this route by a quinone, which could result in a photoprotective cyclic pathway<sup>37</sup>.

The cytochrome- $b_6f$  complex

The isolation of the chloroplast cytochrome- $b_6f$  complex highlighted its similarity to the mitochondrial cytochrome- $bc_1$  complex<sup>14</sup>. Cloning the genes that

encode cytochrome- $bc_1$  subunits from mammals, birds, yeast and different bacteria indicated that they all evolved from a common ancestor, in which **cytochrome b** and the **RIESKE IRON-SULPHUR PROTEIN** were central. In addition, a *c*-type cytochrome is present in most of these cytochrome- $bc_1$  complexes or is found together with these complexes as a separate moiety<sup>38</sup>. All these cytochrome- $bc_1$  complexes are defined as plastoquinone-plastocyanin (or **cytochrome c**) oxidoreductases, and they generate a pmf force using a mechanism that is known as the **Q CYCLE**<sup>39,40</sup>. In the chloroplast cytochrome- $b_6f$  complex (FIG. 3a), the two-electron oxidation of a reduced quinone ( $PQH_2$ ) that is bound at the luminal  $Q_o$  site results in the release of two protons to the aqueous lumen (FIG. 3b). One electron is transferred from the reduced quinone to plastocyanin through a high-potential chain that consists of the **Rieske iron-sulphur protein** and **cytochrome f**; whereas the second electron is translocated across the membrane, through two haem groups ( $b_L$  and  $b_H$ ) of **cytochrome  $b_6$** , to reduce a quinone that is bound at the stromal  $Q_i$  site. Following a second reduction event at the  $Q_i$  site, two protons are taken up from the stroma at this site and the reduced quinone is released into the lipid bilayer to join the reduced quinone pool. Therefore, a pmf is formed across the membrane<sup>39-41</sup>. The crystal structures of dimeric cytochrome- $bc_1$  complexes from various sources highlighted two large central cavities in which the Q cycle operates and also showed that the Rieske protein must oscillate between its electron-donating site ( $Q_o$ ) and its electron acceptor cytochrome  $c_1$ , which equates to cytochrome  $f$  of the cytochrome- $b_6f$  complex<sup>42-45</sup>.

Each monomer of the dimeric cytochrome- $b_6f$  complex contains four large subunits (of 18–32 kDa) — that is, cytochrome  $f$ , cytochrome  $b_6$ , the Rieske iron-sulphur protein and **subunit IV** — as well as four small

**RIESKE IRON-SULPHUR PROTEIN**  
A subunit of the cytochrome- $bc_1$  and - $b_6f$  complexes that contains an iron-sulphur cluster.

**Q CYCLE**  
The mechanism by which the cytochrome- $bc_1$  and - $b_6f$  complexes achieve their energy transduction to generate a protonmotive force.

**CHLOROPHYLL TRIPLET**  
A chlorophyll with unpaired valence electrons. It can interact with molecular oxygen to form singlet oxygen. This, in turn, is a highly reactive molecule that might destruct nearby proteins or other biologically important molecules.

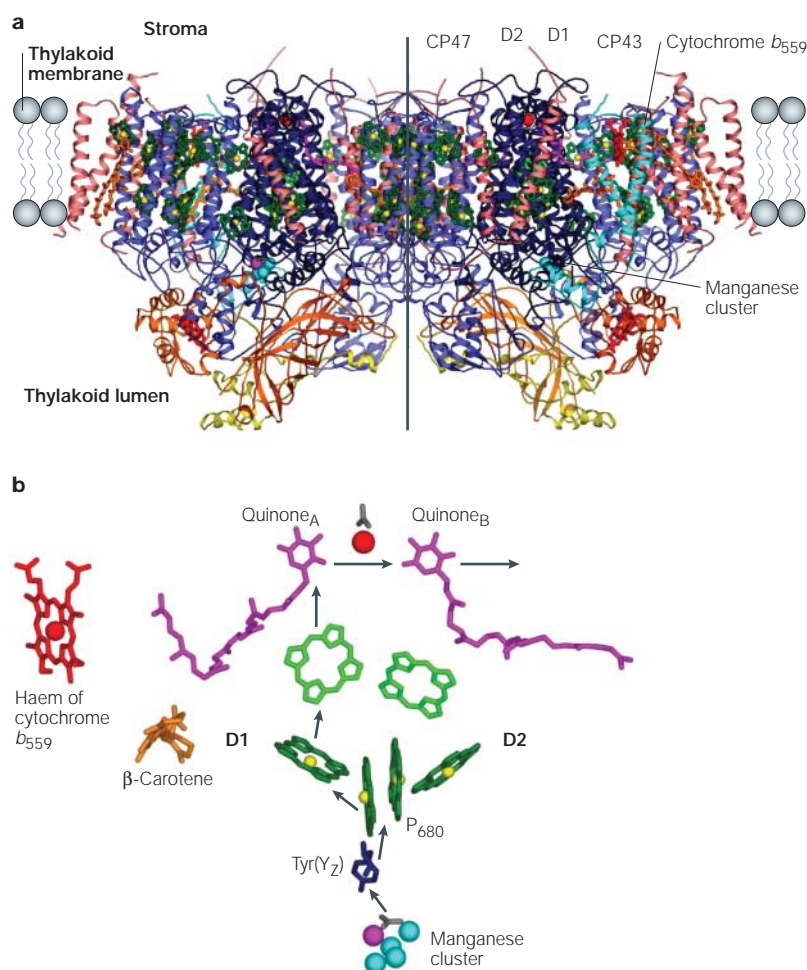


**Figure 2 | The structure of photosystem II and the cofactors that are involved in light-induced water oxidation and plastoquinone reduction.** **a** | A view of the photosystem II (PSII) dimer perpendicular to the membrane normal. The coordinates of protein residues, chlorophylls and cofactors were taken from the Protein Data Bank file 1S5L (REF. 24). The D1 and D2 subunits are shown as dark-blue ribbon structures, CP43 and CP47 as purple ribbon structures, the cytochrome- $b_{559}$  subunits as light-blue ribbon structures, and extrinsic subunits as both orange and yellow ribbon structures. The remaining subunits are shown as light-pink ribbon structures. Chlorophylls are shown in a dark-green stick representation (with the central magnesium ions shown as yellow spheres). The oxygen-evolving complexes/manganese clusters are shown as light-blue spheres (manganese ions) and dark-pink spheres (calcium ions). Haem groups are shown in a red stick representation, and red spheres represent iron ions. Orange stick-like structures represent  $\beta$ -carotene, and dark-pink stick-like structures represent the quinones. The axis of symmetry of the dimer is highlighted by a line. **b** | The cofactors that are involved in electron transport in PSII are shown in the same positions as in the left part of the PSII dimer in FIG. 2a. The arrows indicate the electron-transport pathway to the photooxidized  $P_{680}$  (two weakly coupled chlorophylls that function as the primary electron donor) and to the oxidized quinone. The colour scheme is the same as for part **a**, with the addition of pheophytins in light green, tyrosine 161 of D1 — Tyr( $Y_z$ ) — in dark blue and bicarbonate ions in grey. The chlorophyll molecules are represented by symmetrical porphyrins.

#### STATE TRANSITION

A short-term response to light conditions, in which plants can differentially distribute light energy between photosystem I and photosystem II. It is thought to occur through the relocation of light-harvesting complex II between the two photosystems.

hydrophobic subunits (PetG, PetL, PetM and PetN). This leads to a dimer that has a molecular weight of 217 kDa (REFS 46,47). Cytochrome  $b_6$  and subunit IV are homologous to the N- and C-terminal halves, respectively, of cytochrome  $b$  of the cytochrome- $bc_1$  complex. The Rieske iron-sulphur proteins of the cytochrome- $b_6f$  and cytochrome- $bc_1$  complexes are also similar<sup>48</sup>. However, the  $c$ -type cytochrome  $f$  of the cytochrome- $b_6f$  complex is unrelated to cytochrome  $c_1$  of the  $bc_1$

complex<sup>49</sup>. Remarkably, two cofactors of unknown function — chlorophyll- $a$  and  $\beta$ -carotene — are also part of the cytochrome- $b_6f$  complex<sup>49</sup> (FIG. 3a).

The crystal structures of the cytochrome- $b_6f$  complexes from *Mastigocladus laminosus* and *Chlamydomonas reinhardtii* indicate that they are dimers (FIG. 3), the organizations of which are similar to that of cytochrome  $bc_1$ . However, the extramembrane domains of cytochrome  $f$  and the Rieske protein, which lie on the luminal side of the membrane, are shifted considerably in comparison to their counterparts in the cytochrome- $bc_1$  complex<sup>46,47</sup>. Furthermore, PetG, PetL, PetM and PetN have no parallels in cytochrome- $bc_1$ . Conversely, helix H of cytochrome  $b$  and the small subunits su10, su7 and su11 of cytochrome  $bc_1$  have no equivalents in the cytochrome- $b_6f$  complex. The small subunits of cytochrome  $b_6f$  occupy a site that is partially filled with a specific lipid in cytochrome  $bc_1$ , so they might therefore function as space fillers. The chlorophyll- $a$  and  $\beta$ -carotene cofactors might have a similar space-filling function. The recent structure of the *C. reinhardtii* cytochrome- $b_6f$  complex now provides us with the opportunity to generate directed amino-acid substitutions that might address some of the intriguing questions that remain to be answered, such as why the chlorophyll- $a$  cofactor does not fluoresce, and how photons that are absorbed by this chlorophyll are quenched without generating dangerous CHLOROPHYLL TRIPLETS.

The presence of a further haem group that is covalently bound to cytochrome  $b_6$  is also puzzling<sup>46,47</sup>. The extra haem is located at the stromal face between the  $b_H$  haem group and the  $Q_i$  site (FIG. 3). The existence of this extra haem at a position that is accessible from the stroma gives credence to the idea that ferredoxin might be able to transfer electrons directly to an oxidized quinone at the  $Q_i$  site of cytochrome  $b_6f$ , as part of the process of cyclic photophosphorylation (FIG. 1b). Cyclic photophosphorylation is an alternative electron-transfer pathway that, unlike the prevailing linear mode, does not involve PSII. In this process, a pmf is formed by electrons that flow from PSI through a quinone and the cytochrome- $b_6f$  complex back to PSI. No NADPH is formed in this pathway and its molecular basis and regulation are ill-defined.

The redox state of the quinone pool — that is, the proportion of reduced versus oxidized quinones — regulates both short-term and long-term responses to an imbalance in the activities of the two photosystems<sup>50–53</sup>. The cytochrome- $b_6f$  complex functions as the sensor of this redox state and therefore has a key role in the acclimatization of the photosynthetic apparatus to the varying environment. In 'STATE TRANSITION', one of the short-term responses that is regulated by cytochrome  $b_6f$  — the binding of  $PQH_2$  to the  $Q_o$  site — was shown to control the activation of a stromal kinase that probably carries the signal further through a cascade of kinases<sup>54–56</sup>. The most intriguing question in terms of the role of cytochrome  $b_6f$  in this process is how the binding of the reduced quinone at the luminal  $Q_o$  site is conveyed to the stromal signal-transduction machinery. The chlorophyll in the cytochrome- $b_6f$

complex<sup>47</sup> or conformational changes that result from the oscillation of the Rieske centre<sup>57</sup> were proposed to fulfill this task, but no clear answer has been obtained. The recent structures of the cytochrome-*b<sub>6</sub>f* complex should prove invaluable in helping to shed light on this issue.

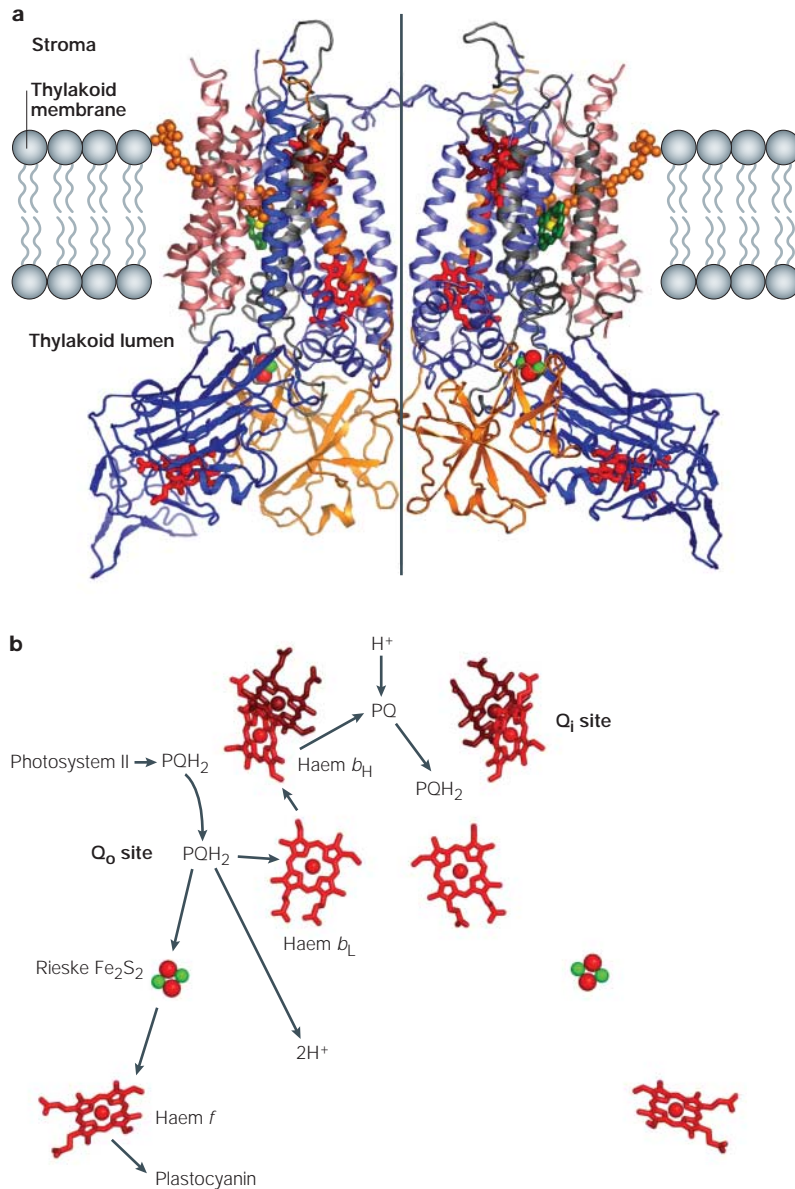


**Figure 3 | The structure of the cytochrome-*b<sub>6</sub>f* complex from *Chlamydomonas reinhardtii* and the cofactors that are involved in its mechanism of action. **a** | A view of the cytochrome-*b<sub>6</sub>f* complex dimer perpendicular to the membrane normal. The axis of symmetry of the dimer is highlighted by a line. The coordinates of the protein residues and cofactors were taken from the Protein Data Bank file 1O90 (REF. 47). The cytochrome-*b<sub>6</sub>* subunits are shown as purple ribbon structures, the subunit IV subunits as grey ribbon structures, Rieske iron–sulphur proteins are shown as orange ribbon structures and cytochrome-*f* subunits are shown as dark-blue ribbon structures. The small subunits (PetG, PetL, PetM and PetN) are shown as light-pink ribbon structures. Haems *b<sub>H</sub>*, *b<sub>L</sub>* and *f* are shown in a red stick representation (the central red spheres represent iron ions), and the extra haems are shown in dark red. Orange spacefill structures represent  $\beta$ -carotene, chlorophylls are shown in a dark-green stick representation (with the central magnesium ions shown as yellow spheres), and iron–sulphur clusters are represented by red and green spheres. **b** | The cofactors that are involved in electron transport are shown in the same positions as in FIG. 3a. The arrows indicate the electron transport that occurs during the Q cycle of plastoquinone (PQ)–plastocyanin oxidoreduction and the proton transport activity of the complex. The extra haems (dark red) are not directly involved in the Q cycle.**

### Photosystem I

PSI of higher plants is composed of two moieties: a reaction centre and the peripheral light-harvesting complex I (LHCI; FIG. 4). The reaction centre comprises 12–14 subunits that are denoted PsaA–PsaL, PsaN and PsaO. The PsaA–PsaB heterodimer forms the heart of PSI. It binds the P<sub>700</sub> special chlorophyll pair, which is where the light-driven charge separation occurs, and it also includes the primary electron acceptors A<sub>0</sub> (chlorophyll-a), A<sub>1</sub> (phylloquinone) and F<sub>X</sub> (an Fe<sub>4</sub>-S<sub>4</sub> cluster; FIG. 5). In addition, this heterodimer coordinates ~80 chlorophylls that function as an intrinsic light-harvesting antenna<sup>58,59</sup>. The terminal components of the electron-transfer chain — that is, two further Fe<sub>4</sub>-S<sub>4</sub> clusters (F<sub>A</sub> and F<sub>B</sub>) — are bound to PsaC. The rest of the subunits participate in the docking of ferredoxin (PsaC, PsaE and PsaD) and plastocyanin (PsaF), the association with LHCI (PsaK, PsaG, PsaJ and PsaF), the docking of LHCII (PsaI, PsaH and PsaL) and the maintenance of complex integrity, and they probably also have other functions<sup>60</sup>.

Like all the other protein complexes that carry out oxygenic photosynthesis, PSI is present in cyanobacteria, algae and plants. The core of the PSI reaction centre is highly conserved in these organisms, and it is therefore assumed that a similar structure existed at the dawn of oxygenic photosynthesis more than three billion years ago<sup>61</sup>. As was shown by the crystal structures of cyanobacterial and plant PSI<sup>59,62</sup>, the bulk of the reaction centre is built of two, homologous, large subunits (PsaA and PsaB) that harbour most of the PSI pigments and all of the cofactors that are involved in light-induced electron transfer from the special, tightly-coupled, chlorophyll pair (P<sub>700</sub>) to the electron acceptor F<sub>X</sub><sup>59</sup>. Therefore, a basic pseudo-twofold-symmetry structure dominates the central core of PSI<sup>63</sup>. The evolution of PSI was probably initiated over 3.5 billion years ago by the formation of a homodimeric reaction centre that is similar to the one found today in green bacteria<sup>38,64–67</sup>. Gene duplication probably generated a heterodimeric reaction centre that subsequently evolved into the PSI that is now found in cyanobacteria, and in the chloroplasts of algae and plants<sup>63</sup>.

Oxygenic photosynthesis operates under vastly different conditions, which are dictated by the ecological niches that different organisms occupy. Whereas green algae and plants are mainly present on the surface of oceans and on land, cyanobacteria usually proliferate deep in oceans and other bodies of water. Consequently, they are protected from high light intensities and must compete for the dim light of their environment<sup>68</sup>. This has led to the formation of several specific light-harvesting complexes in cyanobacteria, such as phycobilisomes that absorb the green light that filters through the green algae on the surface. A life at low light intensities probably drove the formation of the trimeric PSI that is present in cyanobacteria<sup>69,70</sup>.

The plant PSI uses an extrinsic, peripheral light-harvesting membrane antenna (LHCI), and this antenna is composed of a modular arrangement of four light-harvesting chlorophyll-containing proteins

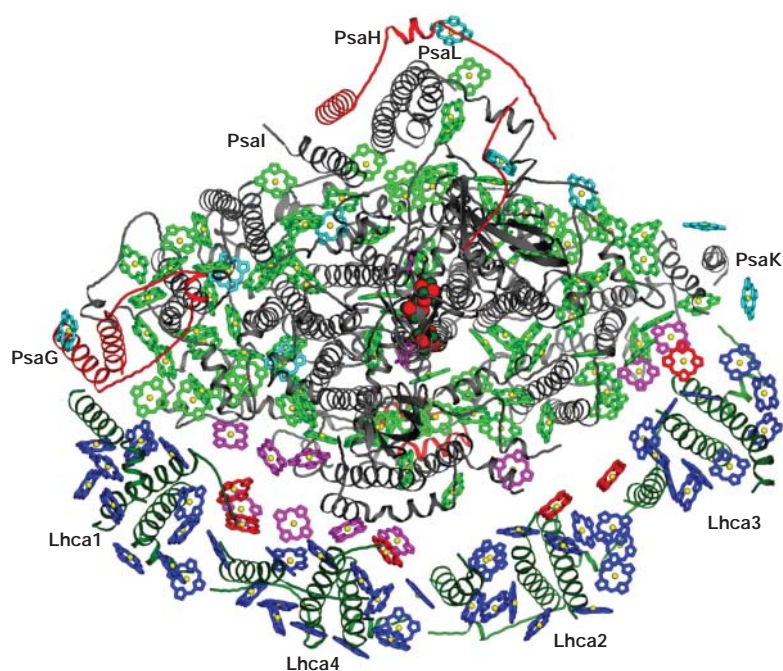


**Figure 4 | A view from the stroma on plant photosystem I.** A view from the stroma of the structure of plant photosystem I (PSI). The structural coordinates for PSI were taken from the Protein Data Bank file 1OZV (REF. 62). The  $C_{\alpha}$  backbones of the light-harvesting proteins are shown as dark-green ribbon structures. Novel structural elements in the reaction centre of PSI that are not present in the cyanobacterial counterpart are shown as red ribbon structures, and the conserved features of the reaction centre are shown as grey ribbon structures. The three  $Fe_4S_4$  clusters are represented by red and green spheres. The colour code for the chlorophyll molecules (in which the central magnesium ions are shown as yellow spheres) is: green, plant reaction-centre chlorophylls that are present in cyanobacteria; light blue, reaction-centre chlorophylls that are unique to plants; dark blue, chlorophylls that are bound to the light-harvesting complex I (LHCI) monomers (Lhca1–Lhca4); red, LHCI ‘linker’ chlorophylls; and dark pink, chlorophylls that are positioned in the cleft between LHCI and the reaction centre. The reaction centre comprises 12–14 subunits that are denoted PsaA–PsaL, PsaN and PsaO, and some of these subunits are labelled in this figure.

(Lhca1–Lhca4). The recently determined structure of plant PSI (FIGS 4.5) showed that the four Lhca proteins assemble into two dimers that form a crescent-shaped belt that docks to the PsaF side of the reaction centre<sup>62</sup>. One of the striking features of this arrangement is that relatively weak interactions have a key role in establishing the LHCI belt and its association with the reaction centre (FIGS 4.5). Binding between the Lhca proteins does not involve any helix–helix interactions. Solvent-exposed N- and C-terminal tails protrude out of the main body of each Lhca monomer and attach to luminal and stromal regions of the neighbouring monomer through relatively small binding surfaces. This creates a sort of head-to-tail arrangement, which maximizes the number of chlorophylls that face the reaction centre, but leaves large distances between the chlorophylls of neighbouring Lhca monomers<sup>62,71</sup>. These distances are bridged by strategically positioned ‘linker chlorophylls’ between the Lhca monomers (FIG. 4).

The association of LHCI with the reaction centre is asymmetric in the sense that only one monomer, Lhca1, binds tightly to the reaction centre, through a helix bundle that is formed with PsaG (FIG. 4). The other Lhca

monomers attach to the reaction centre through relatively weak interactions that mainly involve stromal domains and through their association with the neighbouring monomer<sup>62,71</sup>. So, the strongly bound Lhca1 or the Lhca1–Lhca4 dimer form an anchor point for the assembly and stability of Lhca. This mode of association between the reaction centre and LHCI, as well as the flexible binding between Lhca monomers, provides the structural basis that explains how the composition of LHCI might be dynamically altered as a function of light intensity or nutrient availability. *Arabidopsis thaliana* plants that are grown under different light intensities show sharp fluctuations in their Lhca2 and Lhca3 levels<sup>72</sup>. On the other hand, the level of Lhca4 is modified (drops sharply) only under high light intensities, and the amount of Lhca1 remains constant at all intensities. This flexible or modular nature of the LHCI antenna is probably essential to allow plants to adjust to varying light intensities<sup>72,73</sup>.

There are other important consequences of these modes of interaction<sup>62</sup>. Within the membrane, a 20-Å-wide cleft is formed between LHCI and the reaction centre. Most LHCI chlorophylls are 20–30 Å from the nearest reaction-centre chlorophyll, but there are two major and one minor ‘contact regions’ where much shorter inter-pigment distances are observed (10–15 Å). These regions might therefore represent preferred routes for energy flow from LHCI to the reaction centre<sup>71,74,75</sup>.

Photosynthetic organisms have developed several mechanisms to cope with various stress conditions. A recently identified example is the formation of a large, transmembrane antenna complex — which is composed of 18 monomers of a CP43-like protein — around the PSI trimer in cyanobacteria under iron-deprivation conditions<sup>76,77</sup>. Plants had to develop unique mechanisms to acclimatize to the varying environmental conditions on land. One such response to alterations in light properties — state transition — involves the rapid (within minutes) redistribution of absorbed energy between PSII and PSI. When excess light is captured by PSII, a subpopulation of LHCII trimers dissociates from PSII and associates with PSI<sup>50,51</sup>. This response correlates with the activity of a kinase that phosphorylates LHCII, although the role of this phosphorylation is not yet clear<sup>78,79</sup>. PSI that is defective in PsaH is deficient in state transition, and crosslinking studies have indicated that the docking site for LHCII is formed by the subunits PsaI, PsaL and PsaH<sup>80,81</sup> (FIG. 4).

The cyanobacterial PSI is trimeric both *in vitro* and *in vivo*. Disruption of PsaL in cyanobacterial PSI prevented trimer formation and the mutant cells showed reduced growth under low light intensities<sup>69</sup>. On the other hand, PSI of plants and algae is monomeric and its recently elucidated structure shows that this property is advantageous for its operation under fluctuating light intensities<sup>62,63</sup>. The addition of PsaH (which is not present in cyanobacteria) and the truncation, in plants, of the trimer-forming domain of PsaL blocked the ability of plant and algae

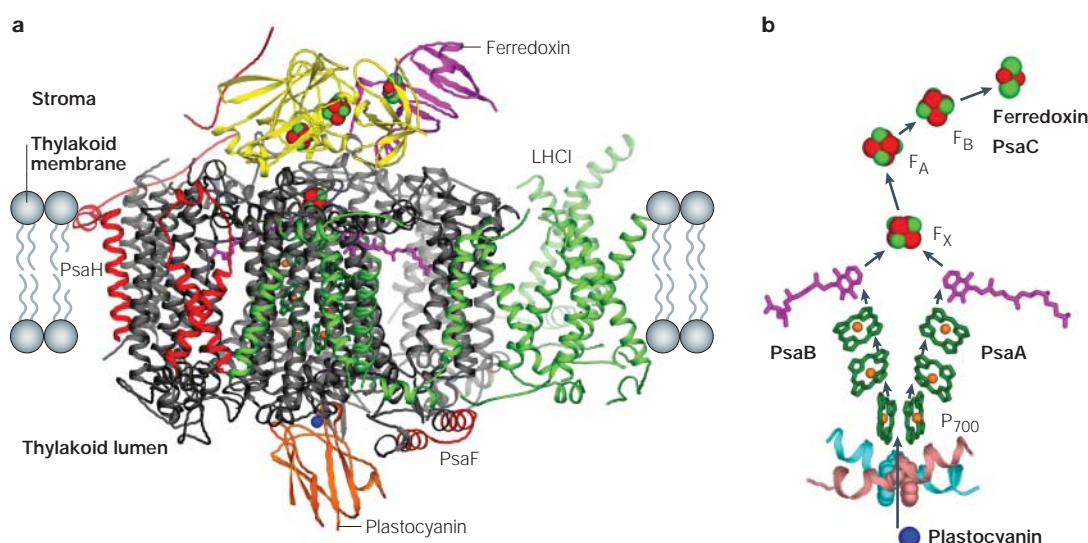


**Figure 5 | A model for the interaction of plant photosystem I with its electron donors/acceptors and the pathways for light-induced electron transport.** **a** | A side view of the putative interactions between plant photosystem I (PSI), plastocyanin and ferredoxin. The structural coordinates for PSI were taken from the Protein Data Bank (PDB) file 1OZV (REF. 62). The coordinates for plastocyanin and ferredoxin were taken from PDB files 1AG6 (REF. 83) and 1A70 (REF. 82), respectively. The reaction centre comprises 12–14 subunits that are denoted PsaA–PsaL, PsaN and PsaO, and two of these subunits are labelled in this figure. The stromal subunits are shown as yellow ribbon structures, and novel structural elements in the reaction centre that are not present in the cyanobacterial counterpart are shown as red ribbon structures. The conserved features of the reaction centre are shown as grey ribbon structures, and the light-harvesting complex I (LHCI) is shown as a green ribbon structure. The electron-transfer components of PSI are: chlorophylls (dark-green stick representations, in which the central orange spheres represent magnesium ions); quinones (dark-pink stick representations); and three  $\text{Fe}_4\text{S}_4$  clusters that are highlighted by red and green spheres. Plastocyanin is shown as an orange ribbon structure and its copper atom is represented by a blue sphere. Ferredoxin is shown as a dark-pink ribbon structure and its  $\text{Fe}_2\text{S}_2$  cluster is also represented by red and green spheres. **b** | The cofactors that are involved in light-induced electron transport in PSI (REF. 59; PDB file 1JBO). The positions of PsaA, PsaB, PsaC, plastocyanin, ferredoxin and the special chlorophyll pair  $\text{P}_{700}$  are indicated. The colour scheme is the same as for part **a**, and the chlorophyll molecules are represented by symmetrical porphyrins. Two tryptophan residues that might be involved in electron transport from plastocyanin to  $\text{P}_{700}$  are also shown (light-blue and light-pink spacefill structures that are shown in the context of their secondary structural environment).

PSI to form trimers, but enabled the binding of LHCII and therefore the state-transition response.

In addition to the structure of plant PSI, the structures of both its electron donor (plastocyanin) and acceptor (ferredoxin) have also been determined at relatively high resolutions<sup>82,83</sup>, which gives a more complete picture of the charge-transfer mechanism of PSI. Moreover, the structure of the complex that is formed by ferredoxin–NADP reductase (which is known to be bound to PSI) and ferredoxin is also available<sup>84</sup>. FIGURE 5a depicts a model of a super-complex that contains PSI, plastocyanin and ferredoxin. Under certain conditions the reduced ferredoxin might leave its binding site to donate its electron directly to the cytochrome- $b_6/f$  complex and therefore facilitate ATP formation through cyclic phosphorylation (FIG. 1b).

One of the conclusions that could immediately be drawn from the published structures of PSI and PSII is that — as was predicted before<sup>85</sup> — they share fundamental architectural features<sup>38</sup>. The central C-terminal domains of PsaA and PsaB in PSI, which harbour the initial electron-transfer components (from  $\text{P}_{700}$  to  $\text{F}_X$ ), show the same helical arrangement that is observed for D1 and D2 of PSII. Similarly, the N termini of PsaA and PsaB resemble the intrinsic light-harvesting subunits of PSII (CP43 and CP47) in sequence, structure and

pigment content. Perhaps even more striking is the fact that, in both photosystems, the electron-transfer components are arranged in two branches, in which pairs of cofactors are related by a pseudo-twofold-symmetry axis that is perpendicular to the membrane (FIGS 2b,5b). It therefore became clear that the two photosystems are derived from a common ancestor<sup>38</sup>.

However, whereas PSII produces the strongest oxidizing potential in any biological system, the task of PSI is to supply the cell with strong reducing equivalents. Furthermore, in PSI, the last electron acceptor is an iron–sulphur protein that is oxidized and reduced by a single electron during every light cycle (FIG. 5b). In PSII, this role is taken by a quinone that, after being reduced twice, takes up two protons from the stroma and dissociates from PSII (FIG. 2b). So, although they share general design principles, the two photosystems must provide essentially different environments for their cofactors. This is evident in the chlorophyll content of the central domain. In PSI, nearly 50 chlorophylls are 20–30-Å away from the electron-transport chain and these chlorophylls might provide the special chlorophyll pair ( $\text{P}_{700}$ ) with excitation energy<sup>59,62</sup>. In sharp contrast, the central domain of PSII contains only two light-harvesting chlorophylls. This, and the fact that there are no protective carotenoids in the vicinity of  $\text{P}_{680}$ , might be because

of the devastatingly high potential that is produced by  $P_{680}$ , which might oxidize any pigments in its proximity<sup>24</sup>. These differences are manifested in the fact that there is no sequence similarity between D1–D2 and the core domain of PsaA–PsaB, despite the structural resemblance. The relatively low quantum yield of PSII might be mostly due to this lack of chlorophylls in the core domain, and also due to features that are common to reaction centres that have a mobile quinone as their last acceptor. Another fundamental difference between PSI and PSII lies in the fact that, in PSII, only one of the electron-transfer branches is active, whereas electrons are translocated by both branches in PSI, albeit at different rates<sup>86</sup> (FIGS 2b,5b). PSII cannot use this bidirectional electron transfer, as it would take longer, on average, for the same quinone to be reduced twice, and would therefore increase the risk of back transfer from a singly reduced quinone to  $P_{680}$ . The structure of the cyanobacterial PSI revealed several features that might account for the uneven electron-transfer rate along the two branches<sup>59</sup>. However, the structural features that are responsible for this phenomenon need to be confirmed, and the biological advantages that this confers need to be determined.

The ATP synthase (F-ATPase)

ATP synthase (F-ATPase) is ubiquitously found on energy-transducing membranes, such as chloroplast thylakoid membranes, mitochondrial inner membranes and bacterial plasma membranes. In cyanobacteria and the chloroplasts of algae and plants, this enzyme catalyses ATP synthesis using a transmembrane pmf that is generated by the photosynthetic electron-transport chain<sup>15</sup>. The general structural features of the chloroplast F-ATPase are highly conserved, and its structure and mechanism are similar to those of bacterial and mitochondrial F-ATPases<sup>87</sup>. The enzyme is a multisubunit complex with distinct stromal and transmembrane regions that are known as  $CF_1$  and  $CF_0$ , respectively, and it represents a molecular motor that is driven by a pmf. Proton movement through  $CF_0$  is coupled to ATP synthesis/hydrolysis at sites in the  $\beta$ -subunits of  $CF_1$ . In chloroplasts,  $CF_0$  contains four subunits I, II, III and IV in a probable stoichiometry of 1:1:14:1. The 14 III subunits form a ring-like structure that is equivalent to the c-ring of other F-ATPases<sup>15</sup>. The whole  $CF_0$ – $CF_1$  complex is thought to function as a rotary proton-driven motor, in which the stationary subunits are I, II, IV,  $\delta$ ,  $\alpha$  and  $\beta$ , and the rotary subunits are III (c),  $\gamma$  and  $\epsilon$  (FIG. 6).

The crystal structure of the bovine mitochondrial  $F_1$ -ATPase showed an alternating arrangement of three  $\alpha$ -subunits and three  $\beta$ -subunits around the central, helical, coiled-coil  $\gamma$ -subunit<sup>88</sup>. The structure strongly supported the binding-change mechanism that was proposed by Boyer<sup>89</sup>, which is a mechanism that involves alternating conformational changes in the nucleotide-binding sites of the catalytic  $\beta$ -subunits. The binding of protons to the c-subunit drives the rotation of the c-ring and the central stalk ( $\gamma$ - and  $\epsilon$ -subunits) that is physically attached to the ring. The rotation of the stalk induces alternating conformational changes in the nucleotide-binding sites of the catalytic  $\beta$ -subunits,

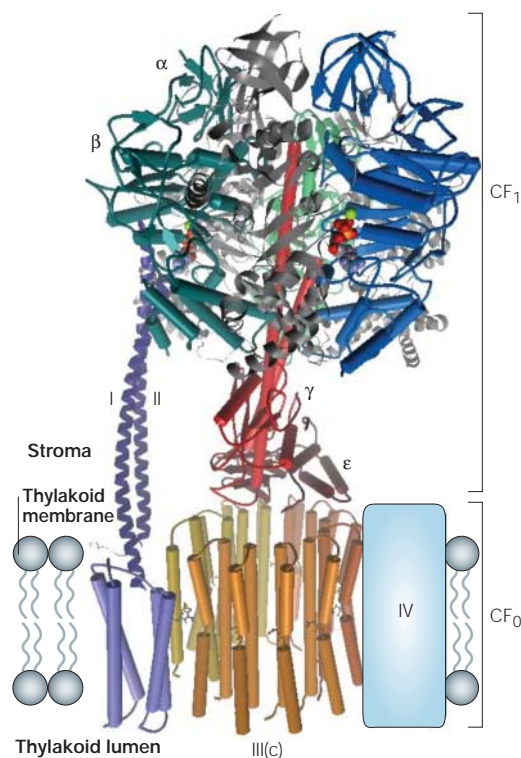


**Figure 6 | A composite model for the structure of the chloroplast F-ATPase.** This model was created by W. Frasch (Arizona State University, Arizona, USA) using available structural data for mitochondrial F-ATPase subcomplexes (REFS 88,90,91), as well as biochemical information. The missing subunit IV has been added in a schematic form, whereas the  $\delta$  subunit is not shown because its exact location is unclear. Only one of the three  $\alpha$ -subunits and one of the three  $\beta$ -subunits are labelled, and the green, grey and blue shading of the  $\alpha$ - and  $\beta$ -subunits highlights three different conformations. It is thought that the c/III-ring contains 14 c/III-subunits, rather than 12 as shown in this figure.

the rotation of which is prevented by the stator (stationary) subunits I and II. Therefore, a complete cycle of the rotor yields three ATP molecules. The structure of the central stalk of an intact  $F_1$ -domain has recently been determined to a high resolution<sup>90</sup>, and the structure of the yeast  $F_1$ -domain attached to a ring of 10 c-subunits has also been solved to 3.9-Å resolution<sup>91</sup>. The close contact between the  $\gamma$ - and  $\epsilon$ -subunits and the c-ring supports the idea that this central stalk and the c-ring form the rotary ensemble of the ATPase motor. Models for rotation of the stalk have been proposed in which the ring of c-subunits rotates past a fixed a-subunit (subunit IV in chloroplasts)<sup>92,93</sup>. FIGURE 6 depicts a model for the structure of the chloroplast F-ATPase that was assembled from crystal structures of partial complexes of the mitochondrial F-ATPase<sup>88,90,91</sup>. The chloroplast F-ATPase resembles that of mitochondria, but shows significant unique features. Recent structural data from yeast<sup>93</sup> and plants<sup>94</sup> indicate that there are 10 and 14 c/III-subunits per F-ATPase complex, respectively. This has come as a surprise, as it was widely anticipated that the number of c/III-subunits would be fixed and would probably be 12 (REF. 95). The finding that the number of c/III-subunits is not divisible by three indicates

that the number of protons that are translocated through the membrane per ATP produced is not an integer and is species specific. So, in yeast mitochondria,  $10/3 = 3.3$  protons are required for the formation of one ATP molecule and, in chloroplasts,  $14/3 = 4.6$  protons are needed<sup>91,94</sup>.

The discovery that there are 14 c/III-subunits in CF<sub>0</sub> of F-ATPase might also finally resolve the long-standing debate that concerns the importance of the *in vivo* cyclic phosphorylation that supplies the CALVIN CYCLE with extra ATP<sup>96</sup>. The assimilation of carbon dioxide by the Calvin cycle requires an ATP:NADPH ratio of 3:2. Formerly, it was calculated that the 4 electrons that are extracted from water produce 2 NADPH molecules and pump 12 protons across the membrane, which would then drive one full cycle of the F-ATPase to yield the required 3 ATP molecules. This calculation is no longer valid in view of the 14 c/III-subunits in the CF<sub>0</sub> ring. An alternative pathway, with no net electron transfer, must therefore supply the two extra protons that are needed. Cyclic electron transfer around PSI is the most probable candidate for this pathway<sup>96</sup>. This idea is given credence by the recent finding that PSI absorbs ~20% more photons than PSII<sup>97</sup>. Therefore, the surplus quanta must be used by alternative pathways, notably, cyclic phosphorylation. Moreover, in the specialized tissues (for example, the bundle sheath) of certain plants such as maize, cyclic phosphorylation comprises nearly the entire photosynthetic process, as there is almost no PSII present (for a review, see REF. 16).

In addition to allowing the synthesis of the necessary ATP, the  $\Delta$ pH that is formed by cyclic phosphorylation might have an important role in protection against the possible damages of high light intensities that exceed the capacity of the reaction centres<sup>98</sup>. Under high light intensities, the build-up of a  $\Delta$ pH across the thylakoid membrane by the prevailing linear electron-transfer pathway triggers, within minutes, a process that switches the PSII antenna into a quenching state, such that most of the absorbed energy is dissipated as heat by a process that is known as non-photochemical quenching (NPQ; REFS 99, 100). The resulting downregulation of PSII, and therefore of linear electron transfer, means that cyclic electron transfer around PSI is now needed both to accept the electrons that keep coming from PSI and to maintain the  $\Delta$ pH and the NPQ process that are protecting PSII. A mutant that is defective in cyclic electron transfer was indeed shown to be deficient in NPQ and it showed elevated fluorescence levels under high light intensities<sup>98</sup>. This higher fluorescence level, which indicates that a smaller proportion of the excess light was dissipated as heat, was used to isolate the mutant. Recently, it was shown that complete elimination of the cyclic electron-transfer pathway around PSI severely impairs the photoautotrophic capability of higher plants<sup>101</sup>. The fact that photosynthesis was impaired even under low light intensities indicates that the main role of cyclic phosphorylation is to provide sufficient ATP and to adjust the ATP:NADPH ratio in the stroma.

The unique features of the chloroplast F-ATPase are the 14-subunit c/III-ring of CF<sub>0</sub> and its activation by light, which occurs through the thioredoxin-mediated

reduction of a disulphide bond in the  $\gamma$ -subunit of CF<sub>1</sub>. So, in addition to supplying the energy for ATP synthesis, the pmf is necessary to activate the chloroplast F-ATPase<sup>15</sup>. The activity of the enzyme is controlled by a process called thiol modulation, which activates the enzyme in the presence of light through the reduction of a specific disulphide bridge that is located in the  $\gamma$ -subunit<sup>15</sup>. In the available F<sub>1</sub> structure, the domain of the  $\gamma$ -subunit that contains this bond is not well resolved, so there is no clear understanding of the mechanism of thiol modulation in the chloroplast F-ATPase. *In vivo*, the  $\gamma$ -subunit reduction is achieved by a thioredoxin that uses electrons that have been diverted from PSI<sup>102,103</sup>. The presence of the  $\epsilon$ -subunit affects the binding of thioredoxin<sup>104</sup>, and thioredoxin binding to isolated CF<sub>1</sub> causes the release of the  $\epsilon$ -subunit<sup>105</sup>. As the  $\epsilon$ -subunit was shown to be involved in regulating the ATPase activity of CF<sub>1</sub> (REF. 106), and as it is in close contact with the  $\gamma$ -subunit, the oxidation or reduction of a  $\gamma$ -subunit thiol might change the position of the  $\epsilon$ -subunit. So, under oxidizing conditions (in the dark), the movement of the rotary section ( $\gamma$ -subunit) might be restricted by the  $\epsilon$ -subunit, such that the ATPase activity of the enzyme is blocked. However, in the presence of light, the pmf build-up and the increased redox potential — which cause the accumulation of reduced thioredoxin and therefore  $\gamma$ -subunit thiol modulation — might result in the movement of the  $\epsilon$ -subunit to a position that no longer inhibits the activity of the enzyme. However, a three-dimensional structure of the chloroplast F-ATPase is needed to allow us to fully understand the fine differences between this enzyme and its mitochondrial counterpart.

The grand design of photosynthesis

Their lack of motility means that plants need to be able to adjust biochemically to a highly dynamic environment that has variations in temperature, light properties and the availability of essential nutrients. It is remarkable that the activity and composition of the photosynthetic apparatus and its acclimatization to the fluctuating environment is self-regulated — the products and intermediate metabolites of photosynthesis, through feedback and feed-forward loops, control the operation of both the light and dark reactions<sup>107</sup>. We feel that the photosynthetic process therefore provides a unique opportunity for a comprehensive interdisciplinary approach. Photosynthesis is perhaps the only key biological process in which the activity of most of the participating protein complexes can be measured using non-invasive methods and for which the structures of these complexes are known at medium-to-high resolution. We therefore believe that photosynthesis is about to enter a new era, in which understanding how the possible routes for energy flow are balanced, especially under real conditions, becomes the new 'Holy Grail'. One of the key ways that this goal might be achieved is through the characterization and structural determination of supercomplexes that might transiently form in the thylakoid membrane (for example, PSI-cytochrome-*b<sub>6</sub>f*,

#### CALVIN CYCLE

The Calvin cycle is a metabolic pathway that occurs in the stroma of chloroplasts, in which carbon enters in the form of CO<sub>2</sub> and leaves in the form of sugar. The cycle uses ATP as an energy source and NADPH as a reducing agent.

PSI-LHCII and others). X-ray crystallography and electron-microscopy methods would complement one another in elucidating the architecture of these assemblies. The results obtained by using these methods could be synergistically combined with new methods for mapping the ultrastructure of the thylakoid

(such as cryo-electron tomography, atomic-force microscopy, two-dimensional gels, high-throughput yeast two-hybrid systems and protein chips). The research of photosynthesis will therefore remain firmly at the forefront of biological sciences for some time to come.

1. Whatley, F. R., Tagawa, K. & Arnon, D. I. Separation of the light and dark reactions in electron transfer during photosynthesis. *Proc. Natl Acad. Sci. USA* **49**, 266–270 (1963).
2. Hill, R. & Bendall, F. Function of two cytochrome components in chloroplast: a working hypothesis. *Nature* **186**, 136–137 (1960).
3. Duysens, L. N. M., Ames, J. & Kamp, B. M. Two photochemical systems in photosynthesis. *Nature* **190**, 510–514 (1961).
4. Mitchell, P. Coupling of phosphorylation to electron and hydrogen transfer by a chemi-osmotic type of mechanism. *Nature* **191**, 144–148 (1961).
5. McCarty, R. E. & Racker, E. Effect of a coupling factor and its antiserum on photophosphorylation and hydrogen ion transport. *Brookhaven Symp. Biol.* **19**, 202–214 (1966).
6. Jagendorf, A. T. Acid-base transitions and phosphorylation by chloroplasts. *Fed. Proc.* **26**, 1361–1369 (1967).
7. Cramer, W. A. & Butler, W. L. Light-induced absorbance changes of two cytochrome *b* components in the electron-transport system of spinach chloroplasts. *Biochim. Biophys. Acta* **143**, 332–339 (1967).
8. Weber, K. & Osborn, M. The reliability of molecular weight determinations by dodecyl sulfate-polyacrylamide gel electrophoresis. *J. Biol. Chem.* **244**, 4406–4412 (1969).
9. Laemmli, U. K. Cleavage of structural proteins during the assembly of the head of bacteriophage T4. *Nature* **227**, 680–685 (1970).
10. Bengis, C. & Nelson, N. Purification and properties of the photosystem I reaction center from chloroplasts. *J. Biol. Chem.* **250**, 2783–2788 (1975).
11. Bengis, C. & Nelson, N. Subunit structure of chloroplast photosystem I reaction center. *J. Biol. Chem.* **252**, 4564–4569 (1977).
12. Pick, U. & Racker, E. Purification and reconstitution of the N<sub>1</sub> dicyclohexylcarbodiimide-sensitive ATPase complex from spinach chloroplasts. *J. Biol. Chem.* **254**, 2793–2799 (1979).
13. Berthold, D. A., Babcock, G. T. & Yocum, C. F. A highly resolved oxygen-evolving photosystem II preparation from spinach thylakoid membranes. *FEBS Lett.* **134**, 231–234 (1981).
14. Hurt, E. & Hauska, G. A cytochrome *f/b6* complex of five polypeptides with plastoquinol-plastocyanin-oxidoreductase activity from spinach chloroplasts. *Eur. J. Biochem.* **117**, 591–595 (1981).
15. McCarty, R. E., Evron, Y. & Johnson, E. A. The chloroplast ATP synthase: a rotary enzyme? *Annu. Rev. Plant Physiol. Plant Mol. Biol.* **51**, 83–109 (2000).
16. Cramer, W. A. *et al.* Some new structural aspects and old controversies concerning the cytochrome *b<sub>6</sub>f* complex of oxygenic photosynthesis. *Annu. Rev. Plant Physiol. Plant Mol. Biol.* **47**, 477–508 (1996).
17. Junge, W. ATP synthase and other motor proteins. *Proc. Natl Acad. Sci. USA* **96**, 4735–4737 (1999).
18. Herrmann, R. G. Biogenesis and evolution of photosynthetic (thylakoid) membranes. *Biosci. Rep.* **19**, 355–365 (1999).
19. Kafan, D., Brumfeld, V., Nevo, R., Scherz, A. & Reich, Z. From chloroplasts to photosystems: *in situ* scanning force microscopy on intact thylakoid membranes. *EMBO J.* **21**, 6146–6153 (2002).
20. Trissl, H.-W. & Wilhelm, C. Why do thylakoid membranes from higher plants form grana stacks? *Trends Biochem. Sci.* **18**, 415–419 (1993).
21. Barber, J. & Andersson, B. Too much of a good thing: light can be bad for photosynthesis. *Trends Biochem. Sci.* **17**, 61–66 (1992).
22. Anderson, J. M. & Chow, W. S. Structural and functional dynamics of plant photosystem II. *Phil. Trans. R. Soc. Lond. B* **357**, 1421–1430 (2002).
23. Barber, J. Photosystem II: a multisubunit membrane protein that oxidises water. *Curr. Opin. Struct. Biol.* **12**, 523–530 (2002).
24. Ferreira, K. N., Iverson, T. M., Maghlaoui, K., Barber, J. & Iwata, S. Architecture of the photosynthetic oxygen-evolving center. *Science* **303**, 1831–1838 (2004).
25. Kuhlbrandt, W., Wang, D. N. & Fujiyoshi, Y. Atomic model of plant light-harvesting complex by electron crystallography. *Nature* **367**, 614–621 (1994).
26. Liu, Z. *et al.* Crystal structure of spinach major light-harvesting complex at 2.72 Å resolution. *Nature* **428**, 287–292 (2004).
27. Boekema, E. J., van Roon, H., Calkoen, F., Bassi, R. & Dekker, J. P. Multiple types of association of photosystem II and its light-harvesting antenna in partially solubilized photosystem II membranes. *Biochemistry* **38**, 2233–2239 (1999).
28. Nield, J. *et al.* 3D map of the plant photosystem II supercomplex obtained by cryoelectron microscopy and single particle analysis. *Nature Struct. Biol.* **7**, 44–47 (2000).
29. Hoganson, C. W. & Babcock, G. T. A metalloradical mechanism for the generation of oxygen from water in photosynthesis. *Science* **277**, 1953–1956 (1997).
30. Vrettos, J. S., Limburg, J. & Brudvig, G. W. Mechanism of photosynthetic water oxidation: combining biophysical studies of photosystem II with inorganic model chemistry. *Biochim. Biophys. Acta* **1503**, 229–245 (2001).
31. Junge, W., Haumann, M., Ahlbrink, R., Mulikjanian, A. & Clausen, J. Electrostatics and proton transfer in photosynthetic water oxidation. *Philos. Trans. R. Soc. Lond. B* **357**, 1407–1417 (2002).
32. Zouni, A. *et al.* Crystal structure of photosystem II from *Synechococcus elongatus* at 3.8 Å resolution. *Nature* **409**, 739–743 (2001).
33. Kamiya, N. & Shen, J. R. Crystal structure of oxygen-evolving photosystem II from *Thermosynechococcus vulcanus* at 3.7-Å resolution. *Proc. Natl Acad. Sci. USA* **100**, 98–103 (2003).
34. Peloquin, J. M. & Britt, R. D. EPR/ENDOR characterization of the physical and electronic structure of the OEC Mn cluster. *Biochim. Biophys. Acta* **1503**, 96–111 (2001).
35. Robblee, J. H. *et al.* The Mn cluster in the S<sub>0</sub> state of the oxygen-evolving complex of photosystem II studied by EXAFS spectroscopy: are there three Di-μ-oxo-bridged Mn<sub>2</sub> moieties in the tetranuclear Mn complex? *J. Am. Chem. Soc.* **124**, 7459–7471 (2002).
36. Vander Meulen, K. A., Hobson, A. & Yocum, C. F. Calcium depletion modifies the structure of the photosystem II O<sub>2</sub>-evolving complex. *Biochemistry* **41**, 958–966 (2002).
37. Vasil'ev, S., Brudvig, G. W. & Bruce, D. The X-ray structure of photosystem II reveals a novel electron transport pathway between P680, cytochrome *b<sub>559</sub>*, and the energy-quenching cation, CH<sub>1</sub><sup>+</sup>. *FEBS Lett.* **543**, 159–163 (2003).
38. Baymann, F., Brugna, M., Muhlenhoff, U. & Nitschke, W. Daddy, where did (PS)I come from? *Biochim. Biophys. Acta* **1507**, 291–310 (2001).
39. Mitchell, P. Possible molecular mechanisms of the proton-motive function of cytochrome systems. *J. Theor. Biol.* **62**, 327–367 (1976).
40. Trumppower, B. L. The proton-motive Q cycle. Energy transduction by coupling of proton translocation to electron transfer by the cytochrome *b<sub>6</sub>f* complex. *J. Biol. Chem.* **265**, 11409–11412 (1990).
41. Berry, E. A., Guergova-Kuras, M., Huang, L.-S. & Crofts, A. R. Structure and function of cytochrome *bc* complexes. *Annu. Rev. Biochem.* **69**, 1005–1075 (2000).
42. Iwata, S. *et al.* Complete structure of the 11-subunit bovine mitochondrial cytochrome *bc<sub>1</sub>* complex. *Science* **281**, 64–71 (1998).
43. Kim, H. *et al.* Inhibitor binding changes domain mobility in the iron-sulfur protein of the mitochondrial *bc<sub>1</sub>* complex from bovine heart. *Proc. Natl Acad. Sci. USA* **95**, 8026–8033 (1998).
44. Zhang, Z. *et al.* Electron transfer by domain movement in cytochrome *bc<sub>1</sub>*. *Nature* **392**, 677–684 (1998).
45. Hunte, C., Koepke, J., Lange, C., Rossmannith, T. & Michel, H. Structure at 2.3 Å resolution of the cytochrome *bc<sub>1</sub>* complex from the yeast *Saccharomyces cerevisiae* co-crystallized with an antibody Fv fragment. *Structure Fold Des.* **8**, 669–684 (2000).
46. Kurisu, G., Zhang, H., Smith, J. L. & Cramer, W. A. Structure of the cytochrome *b<sub>6</sub>f* complex of oxygenic photosynthesis: tuning the cavity. *Science* **302**, 1009–1014 (2003).
47. Stroebel, D., Choquet, Y., Popot, J. L. & Picot, D. An atypical haem in the cytochrome *b<sub>6</sub>f* complex. *Nature* **426**, 413–418 (2003).
48. Carrell, C. J., Zhang, H., Cramer, W. A. & Smith, J. L. Biological identity and diversity in photosynthesis and respiration: structure of the lumen-side domain of the chloroplast Rieske protein. *Structure* **5**, 1613–1625 (1997).
49. Martinez, S. E., Huang, D., Szczepaniak, A., Cramer, W. A. & Smith, J. L. Crystal structure of chloroplast cytochrome *f* reveals a novel cytochrome fold and unexpected heme ligation. *Structure* **2**, 95–105 (1994).
50. Horton, P. & Black, M. T. Activation of adenosine 5' triphosphate-induced quenching of chlorophyll fluorescence by reduced plastoquinone: the basis of state I-state II transitions in chloroplasts. *FEBS Lett.* **119**, 141–144 (1980).
51. Allen, J. F., Bennett, J., Steinback, K. E. & Arntzen, C. J. Chloroplast protein phosphorylation couples plastoquinone redox state to distribution of excitation energy between photosystems. *Nature* **291**, 25–29 (1981).
52. Escoubas, J. M., Lomas, M., LaRoche, J. & Falkowski, P. G. Light intensity regulation of *cab* gene transcription is signaled by the redox state of the plastoquinone pool. *Proc. Natl Acad. Sci. USA* **92**, 10237–10241 (1995).
53. Pfannschmidt, T., Nilsson, A. & Allen, J. F. Photosynthetic control of chloroplast gene expression. *Nature* **397**, 625–628 (1999).
54. Vener, A. V., Van Kan, P. J., Gal, A., Andersson, B. & Ohad, I. Activation/deactivation cycle of redox-controlled thylakoid protein phosphorylation. Role of plastoquinol bound to the reduced cytochrome *b<sub>6</sub>f* complex. *J. Biol. Chem.* **270**, 25225–25232 (1995).
55. Zito, F. *et al.* The Oo site of cytochrome *b<sub>6</sub>f* complexes controls the activation of the LHCII kinase. *EMBO J.* **18**, 2961–1969 (1999).
56. Depege, N., Bellafiore, S. & Rochaix, J. D. Role of chloroplast protein kinase Stt7 in LHCII phosphorylation and state transition in *Chlamydomonas*. *Science* **299**, 1572–1575 (2003).
57. Wollman, F. A. State transitions reveal the dynamics and flexibility of the photosynthetic apparatus. *EMBO J.* **20**, 3623–3630 (2001).
58. Nelson, N. & Ben-Shem, A. Photosystem I reaction center: past and future. *Photosynth. Res.* **73**, 193–206 (2002).
59. Jordan, P. *et al.* Three-dimensional structure of cyanobacterial photosystem I at 2.5 Å resolution. *Nature* **411**, 909–917 (2001).

**The first high-resolution structure of cyanobacterial PSI, which shows almost all of the amino-acid side chains of its 12 subunits and reveals, in detail, the complete set of electron-transfer components and more than 100 antenna chlorophylls and carotenoids.**

60. Scheller, H. V., Jensen, P. E., Haldrup, A., Lunde, C. & Knoetzel, J. Role of subunits in eukaryotic photosystem I. *Biochim. Biophys. Acta* **1507**, 41–60 (2001).
61. Xiong, J. & Bauer, C. E. Complex evolution of photosynthesis. *Annu. Rev. Plant Biol.* **53**, 503–521 (2002).
62. Ben-Shem, A., Frolow, F. & Nelson, N. The crystal structure of plant photosystem I. *Nature* **426**, 630–635 (2003).  
**The first crystal structure of plant PSI, which contains 16 subunits and 167 chlorophylls. The structure revealed the arrangement of the LHCl belt and its interaction with the reaction centre. It also shed light on the evolutionary forces that shaped plant PSI.**
63. Ben-Shem, A., Frolow, F. & Nelson, N. Evolution of photosystem I — from symmetry through pseudosymmetry to asymmetry. *FEBS Lett.* **564**, 274–280 (2004).
64. Büttner, M. *et al.* Photosynthetic reaction center genes in green sulfur bacteria and in photosystem 1 are related. *Proc. Natl Acad. Sci. USA* **89**, 8135–8139 (1992).
65. Büttner, M. *et al.* The photosystem I-like P840-reaction center of green S-bacteria is a homodimer. *Biochim. Biophys. Acta* **1101**, 154–156 (1992).
66. Hauska, G., Schoedel, T., Remigy, H. & Tsiotis, G. The reaction center of green sulfur bacteria. *Biochim. Biophys. Acta* **1507**, 260–277 (2001).
67. Raymond, J., Zhaxybayeva, O., Gogarten, J. P., Gerdes, S. Y. & Blankenship, R. E. Whole-genome analysis of photosynthetic prokaryotes. *Science* **298**, 1616–1620 (2002).
68. Durnford, D. G. *et al.* A phylogenetic assessment of the eukaryotic light-harvesting antenna proteins, with implications for plastid evolution. *J. Mol. Evol.* **48**, 59–68 (1999).
69. Chitnis, V. P. *et al.* Targeted inactivation of the gene *psaL* encoding a subunit of photosystem I of the cyanobacterium *Synechocystis* sp. PCC 6803. *J. Biol. Chem.* **268**, 11678–11684 (1993).
70. Chitnis, P. R. Photosystem I: function and physiology. *Annu. Rev. Plant Physiol. Plant Mol. Biol.* **52**, 593–626 (2001).
71. Ben-Shem, A., Frolow, F. & Nelson, N. Light harvesting by plant photosystem I. *Photosynthesis Res.* **81**, 239–250 (2004).
72. Bailey, S., Walters, R. G., Jansson, S. & Horton, P. Acclimation of *Arabidopsis thaliana* to the light environment: the existence of separate low light and high light responses. *Planta* **213**, 794–801 (2001).
73. Storf, S., Stauber, E. J., Hippler, M. & Schmid, V. H. Proteomic analysis of the photosystem I light-harvesting antenna in tomato (*Lycopersicon esculentum*). *Biochemistry* **43**, 9214–9224 (2004).
74. Jennings, R. C., Zucchelli, G., Croce, R. & Garlaschi, F. M. The photochemical trapping rate from red spectral states in PSI-LHCI is determined by thermal activation of energy transfer to bulk chlorophylls. *Biochim. Biophys. Acta* **1557**, 91–98 (2003).
75. Morosinotto, T., Breton, J., Bassi, R. & Croce, R. The nature of a chlorophyll ligand in Lhca proteins determines the far red fluorescence emission typical of photosystem I. *J. Biol. Chem.* **278**, 49223–49229 (2003).
76. Bibby, T. S., Nield, J. & Barber, J. Iron deficiency induces the formation of an antenna ring around trimeric photosystem I in cyanobacteria. *Nature* **412**, 743–745 (2001).
77. Boekema, E. J. *et al.* A giant chlorophyll–protein complex induced by iron deficiency in cyanobacteria. *Nature* **412**, 745–748 (2001).
78. Allen, J. F. & Forsberg, J. Molecular recognition in thylakoid structure and function. *Trends Plant Sci.* **6**, 317–326 (2001).
79. Barber, J. Influence of surface charges on thylakoid structure and function. *Annu. Rev. Plant Physiol. Plant Mol. Biol.* **33**, 261–295 (1982).
80. Lunde, C. P., Jensen, P. E., Haldrup, A., Knoetzel, J. & Scheller, H. V. The PSI-H subunit of photosystem I is essential for state transitions in plant photosynthesis. *Nature* **408**, 613–615 (2000).
81. Zhang, S. & Scheller, H. V. Light-harvesting complex II binds to several small subunits of photosystem I. *J. Biol. Chem.* **279**, 3180–3187 (2004).
82. Binda, C., Coda, A., Aliverti, A., Zanetti, G. & Mattevi, A. Structure of the mutant E92K of [2Fe–2S] ferredoxin I from *Spinacia oleracea* at 1.7 Å resolution. *Acta Crystallogr. D Biol. Crystallogr.* **54**, 1353–1358 (1998).
83. Xue, Y., Okvist, M., Hansson, O. & Young, S. Crystal structure of spinach plastocyanin at 1.7 Å resolution. *Protein Sci.* **7**, 2099–2105 (1998).
84. Kurisu, G. *et al.* Structure of the electron transfer complex between ferredoxin and ferredoxin–NADP<sup>+</sup> reductase. *Nature Struct. Biol.* **8**, 117–121 (2001).
85. Schubert, W. D. *et al.* A common ancestor for oxygenic and anoxygenic photosynthetic systems: a comparison based on the structural model of photosystem I. *J. Mol. Biol.* **280**, 297–314 (1998).
86. Guergova-Kuras, M., Boudreaux, B., Joliot, A., Joliot, P. & Redding, K. Evidence for two active branches for electron transfer in photosystem I. *Proc. Natl Acad. Sci. USA* **98**, 4437–4442 (2001).
87. Nelson, N., Sacher, A. & Nelson, H. The significance of molecular slips in transport systems. *Nature Rev. Mol. Cell Biol.* **3**, 876–881 (2002).
88. Abrahams, J. P., Leslie, A. G. W., Lutter, R. & Walker, J. E. Structure at 2.8 Å resolution of F<sub>1</sub>-ATPase from bovine heart mitochondria. *Nature* **370**, 621–628 (1994).  
**The asymmetric structure of the mitochondrial F<sub>1</sub>-ATPase bound to ADP and a non-hydrolysable analogue of ATP. The structure supported the binding-change mechanism for ATP synthesis, which was proposed by Boyer and is reviewed in reference 89.**
89. Boyer, P. D. The ATP synthase — a splendid molecular machine. *Annu. Rev. Biochem.* **66**, 717–749 (1997).
90. Gibbons, C., Montgomery, M. G., Leslie, A. G. W. & Walker, J. E. The structure of the central stalk in bovine F<sub>1</sub>-ATPase at 2.4 Å resolution. *Nature Struct. Biol.* **7**, 1055–1061 (2000).
91. Stock, D., Leslie, A. G. W. & Walker, J. E. Molecular architecture of the rotary motor in ATP synthase. *Science* **286**, 1700–1705 (1999).  
**The structure of the c-ring of the F<sub>0</sub>-ATPase associated with the F<sub>1</sub>-ATPase from yeast showed that the c-ring contains contained ten c-subunits — a number that, contrary to predictions, is not divisible by three.**
92. Engelbrecht, S. & Junge, W. ATP synthase: a tentative structural model. *FEBS Lett.* **414**, 485–491 (1997).
93. Elston, T., Wang, H. Y. & Oster, G. Energy transduction in ATP synthase. *Nature* **391**, 510–513 (1998).
94. Seelert, H. *et al.* Structural biology. Proton-powered turbine of a plant motor. *Nature* **405**, 418–419 (2000).  
**Imaging of the c/III-ring of plant chloroplast F-ATPase using atomic-force microscopy revealed 14 copies of subunit III (c), which indicates that the number of c/III-subunits might vary between organisms.**
95. Girvin, M. E., Rastogi, V. K., Abildgaard, F., Markley, J. L. & Fillingame, R. H. Solution structure of the transmembrane H<sup>+</sup>-transporting subunit c of the F<sub>1</sub>F<sub>0</sub> ATP synthase. *Biochemistry* **37**, 8817–8824 (1998).
96. Joliot, P. & Joliot, A. Cyclic electron transfer in plant leaf. *Proc. Natl Acad. Sci. USA* **99**, 10209–10214 (2002).
97. Danielsson, R., Albertsson, P. A., Mamedov, F. & Styring, S. Quantification of photosystem I and II in different parts of the thylakoid membrane from spinach. *Biochim. Biophys. Acta* **1608**, 53–61 (2004).
98. Munekage, Y. *et al.* PGR5 is involved in cyclic electron flow around photosystem I and is essential for photoprotection in *Arabidopsis*. *Cell* **110**, 361–371 (2002).
99. Li, X. P. *et al.* A pigment-binding protein essential for regulation of photosynthetic light harvesting. *Nature* **403**, 391–395 (2000).
100. Kulheim, C., Agren, J. & Jansson, S. Rapid regulation of light harvesting and plant fitness in the field. *Science* **297**, 91–93 (2002).
101. Munekage, Y. *et al.* Cyclic electron flow around photosystem I is essential for photosynthesis. *Nature* **429**, 579–582 (2004).
102. Buchanan, B. B. & Wolosiuk, R. A. Photosynthetic regulatory protein found in animal and bacterial cells. *Nature* **264**, 669–670 (1976).
103. Mills, J. D. & Mitchell, P. Modulation of coupling factor ATPase activity in intact chloroplasts: reversal of thiol modulation in the dark. *Biochim. Biophys. Acta* **679**, 75–82 (1982).
104. Dann, M. S. & McCarty, R. E. Characterization of the activation of membrane-bound and soluble CF1 by thioredoxin. *Plant Physiol.* **99**, 153–160 (1992).
105. He, X., Migniac-Maslow, M., Sigalat, C., Keryer, E. & Haraux, F. Mechanism of activation of the chloroplast ATP synthase. *J. Biol. Chem.* **275**, 13250–13258 (2000).
106. Nelson, N., Nelson, H. & Racker, E. Partial resolution of the enzymes catalyzing photophosphorylation. XII. Purification and properties of an inhibitor isolated from chloroplast coupling factor I. *J. Biol. Chem.* **247**, 7657–7662 (1972).
107. Anderson, J. M., Chow, W. S. & Park, Y.-I. The grand design of photosynthesis: acclimation of the photosynthetic apparatus to environmental cues. *Photosyn. Res.* **46**, 129–139 (1995).

#### Acknowledgements

We would like to thank W. Frasch for the use of his structural model of F-ATPase (figure 6). A.B.-S. is a recipient of a Charles Clore Foundation Ph.D. student scholarship. The work of N.N. is supported by the Israel Science Foundation.

#### Competing interests statement

The authors declare no competing financial interests.

#### Online links

##### DATABASES

The following terms in this article are linked online to:

**Protein Data Bank:** <http://www.rcsb.org/pdb/1A70|1AG6|1JBO|1O90|1OZV|1S5L>

**Swiss-Prot:** <http://us.expasy.org/sprot/>

human cytochrome *b* | human cytochrome *c*

**TAIR:** <http://www.arabidopsis.org/>

CP24 | CP26 | CP29 | CP43 | CP47 | cytochrome *b<sub>5</sub>* |

cytochrome *f* | D1 | D2 | PetG | PsaA | PsaC | PsaL | PsaJ | Rieske

iron–sulphur protein | subunit IV

Access to this links box is available online.